SIAMOC Best Paper 2021

Superimposition of ground reaction force on tibial-plateau supporting diagnostics and post-operative evaluations in high-tibial osteotomy. A novel methodology☆

Miriana Ruggeri [a], Harinderjit Singh Gill [b], Alberto Leardini [a], Stefano Zaffagnini [c], Alisdair MacLeod [b], Maurizio Ortolani [a], Federica Faccia [a], Alberto Grassi [c], Giacomo Dal Fabbro [c], Stefano Durante [d], Claudio Belvedere [a],*

[a] Movement Analysis Laboratory, IRCCS Istituto Ortopedico Rizzoli, Bologna, Italy
[b] Department of Mechanical Engineering/Centre for Therapeutic Innovation, University of Bath, Bath, UK
[c] II Clinical Department, IRCCS Istituto Ortopedico Rizzoli, Bologna, Italy
[d] Nursing, Technical and Rehabilitation Assistance Service, IRCCS Istituto Ortopedico Rizzoli, Bologna, Italy

ARTICLE INFO

ABSTRACT

Background: A fully personalised combination of Gait Analysis (GA), including Ground Reaction Force (GRF), and patient-specific knee joint morphology has not yet been reported. This can provide valuable biomechanical insight in normal and pathological conditions. Abnormal knee varus results in medial knee condylar hyper-compression and osteoarthritis, which can be prevented by restoring proper condylar load distribution via High Tibial Osteotomy (HTO).

Research question: This study was aimed at reporting on an original methodology, merging GA, GRF and Computer-Tomography (CT) to depict a patient-specific representation of the knee mechanical condition during locomotion. It was hypothesised that HTO results in a lateralized pattern of GRF with respect to the tibial plateau.

Methods: Four patients selected for HTO received clinical, radiological and instrumental examinations, pre- and post-operatively at 6-month follow-up. GA was performed during level walking and more demanding motor tasks using a 9-camera motion-capture system, combined with two force platforms, and an established protocol. Additional skin markers were positioned around the tibial-plateau rim. Weight-bearing CT scans of the knee were collected while still wearing these markers. Proximal tibial and marker morphological models were reconstructed. The markers from CT reconstruction were then registered to the corresponding trajectories as tracked by GA data. Resulting registration matrices were used to report GRF vectors on the plane best matching the tibial-plateau model and the intersection paths were calculated.

Results and significance: The registration procedure was successfully executed, with a max registration error of about 3 mm. GRF intersection paths were found medially to the tibial plateau pre-op, and lateralized post-op, thus much closer to the knee centre, as expected after HTO. The exploitation of the present methodology offers personalised quantification of the original mechanical misalignment and of the effect of surgical correction which could enhance diagnostics and planning of HTO as well as other knee treatments.

1. Introduction

Medial knee osteoarthritis (OA) is generally associated with abnormal varus joint alignment [1], resulting in high compressive loads at the medial tibio-femoral condylar contacts. More specifically, in presence of such impairment, the mechanical axis of the lower limb passes medial to the centre of the knee joint. As a consequence, forces are higher in the medial compartment [2], thus resulting in general medial knee compartmental overloading and cartilage wear [3]. This represents a frequent pathological condition considerably altering the

---

overall locomotion and the load distribution at the two knee compartments [4].

In relatively young patients with early medial OA, i.e. where the cartilage is still not fully compromised, to prevent or delay end-stage disease, misalignment correction is generally considered and frequently performed by High Tibial Osteotomy (HTO) surgery [5–7]. This is a less invasive surgical treatment when compared to total knee arthroplasty, allowing the full preservation of the original tibial plateau morphology. By means of this surgery, in fact, the knee normal alignment is usually restored, with the lower limb mechanical axis thus passing closer to the knee joint centre. As a result, a physiological load distribution within the knee is restored and, in particular, decompression of the medial compartment is achieved thus slowing the mechanism of cartilage deterioration [8].

To evaluate the status of the arthritic knee as well as the efficacy of this and other knee surgeries, a number of pre-operative and post-operative functional and radiological assessments need to be performed. Among them, within standard Gait Analysis (GA), Ground Reaction Force (GRF) and external joint moments can provide relevant information. The three-dimensional (3D) spatial representation of GRF with respect to the lower limb would reflect knee misalignment; this would be far more effective if depicted upon the patient-specific knee morphology. In a varus knee joint for example, the GRF vectors would pass mostly through the medial compartment. External Knee Adduction Moment (KAM) is found to be related to the progression of osteoarthritis and cartilage volume loss: high values correspond to a high degree of arthritis [9,10]. By realigning the tibia and the lower limb mechanical axis, HTO is expected to lateralise the GRF in a more physiologically normal position, thus reducing the peaks of KAM as observed in GA. These analyses would definitely take advantage of thorough integration between gait analysis and medical imaging, by combining bone position and GRF from the former, and bone morphology from the latter. In particular it would be valuable to obtain a superimposition of the GRF vector on subject-specific morphology of the knee. These multi-instrumental evaluations are feasible and have been exploited largely for musculo-skeletal modelling [11,12], but only a few have implied a direct registration of GRF to knee morphology.

By means of a set of reflective markers and stereo-photogrammetric techniques, GA gives as output functional information about the patient's gait patterns, including GRF data and joint moments. However, GA is limited by the missing morphological information of interest. On the other hand, medical imaging techniques are used to easily obtain 2D or 3D images of bones and soft tissues, but the provided information is unrelated to the functional assessments. Therefore, it is important to create a patient-specific connection between functional and morphological data to characterise better joint kinematics and joint loading on a personalised morphological basis. This is fundamental in conservative and surgical treatments, to assess the success of the surgery or to compare the post-operative outcomes with the planning.

Apparently only Whatling et al. [13] has combined GA measurements and morphological information of the knee. The Centre of Pressure (COP) was measured during the first and second half of the stance phase, and registered somehow to the foot and to the knee, based on qualitative illustrations of the plantar aspect of the foot and of the tibial plateau, the latter derived from a previous morphological study from statistical shape analysis [14]. These calculations therefore, were not exactly specific to the morphology of every single knee, nor GRF data was provided.

The primary aim of this study was to report on an original methodology merging GA, including GRF data, and medical imaging in order to depict a realistic patient-specific representation of the knee mechanical condition during locomotion. It could be potentially useful for diagnosis, planning and post-surgery assessment. The secondary aim was to show preliminary applications of such novel methodology on patients selected for HTO. It was hypothesised that, when moving from pre- to post-operative assessments, the pattern of GRF at the tibial plateau level would be shifted laterally and hence, much closer and better aligned to the knee.

2. Materials and methods

2.1. General information

Four patients were analysed (male/female: 2/2; left/right side: 1/3), taken from a larger population within a clinical and biomechanical study. These were affected by early-stage medial knee osteoarthritis resulting from excessive varus, and were indicated for open-wedge HTO. They were fully analysed before the surgery and at 6-month follow-up. Relevant detailed data in mean $\pm$ standard deviation [min$\div$max] for the age, weight, height and Body-Mass-Index (BMI) are, respectively, 46.2 $\pm$ 4.3 [39$\div$50] years, 78.8 $\pm$ 16.2 [58$\div$103] kg, 168.3 $\pm$ 8.6 [156$\div$179] cm, 27.8 $\pm$ 5.8 [23.8$\div$37.8] kg/m^2.

Between December 2019 and March 2021, these patients underwent pre and post-operative radiological and instrumental evaluations, as well as clinical and radiological scoring. The morphological characterisation steps (Fig. 1) included GA and CT acquisitions and were performed before and after HTO. The combination of the pre-operative CT-based 3D model and the radiological images was used to evaluate the degree of deformity and plan the correction and the overall surgery. This particular type of HTO surgery used patient-specific surgical guides and stabilisation plates, for which the geometry was generated from the 3D surgical planning, and then these were 3D printed. This study received institutional review board approval and informed consent was obtained from all individual participants.

2.2. Gait analysis acquisition

GA was performed on patients prior to the surgery and at 6-months follow-up. A 9-camera motion capture system (*Vicon®*, Nexus motion-capture Software v.2.12.1 combined with B10 Bonita Optical cameras, Oxford, UK) together with two force platforms (*Kistler^{TM}*, model 9291B, Winterthur, CH) for GRF tracking was used. In order to reconstruct the position and orientation of the patient's body segments, a set of reflective markers was attached to the skin in well-defined anatomical landmarks, following an established protocol (IOR-gait) [15,16]. To better combine knee motion and subsequent imaging analysis, four 9 mm diameter additional skin-based non-collinear markers were located on the following anatomical landmarks around the tibial plateau bony rim: the most lateral and medial prominences of the tibial plateau (LTibPla, MTibPla), the most distal apex of the patella (PatDis) and a marker was located above the femur lateral epicondyle (LESup) to reconstruct the femur reference frame. Besides traditional level walking, GA was also performed during more demanding activities for the knee i.e., stairs ascending/descending and squatting. Each motor task was repeated at least three times to assess pre-op and post-operative data repeatability.

2.3. Medical imaging procedure

All the analysed patients received pre-operative radiological acquisitions to assess the degree of the deformity and plan the appropriate angle of correction. The same images were acquired after HTO at 6-month follow-up to verify if the desired correction was achieved. These included full lower-limbs X-ray in standing posture, anterior/posterior, 30° lateral and merchant views.

In addition, patients underwent CT scans in weight-bearing. A Cone-Beam CT device (Carestream, Rochester, NY-USA) was used to acquire the knee joint in its natural single-leg standing position with a 0.26 mm resolution. The marker set used in GA was left in situ during this acquisition, thus allowing to create a reference between functional, i.e. GA, and morphological, i.e. 3D imaging, data. The CT scans were used to reconstruct the morphology of the distal femur and the proximal tibia via *Simpleware ScanIP* (version M-2017.06; Synopsys, Inc. Mountain
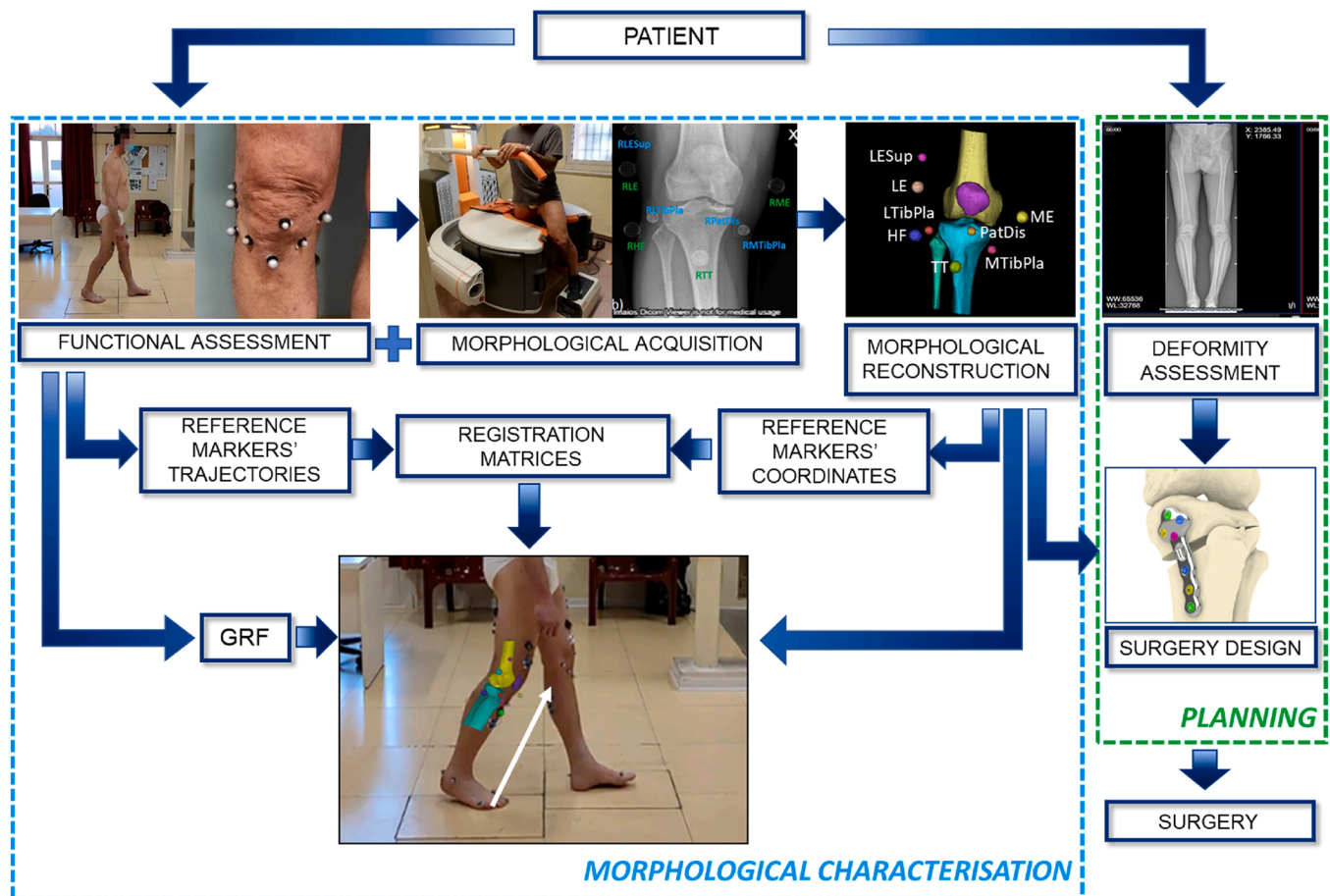
Fig. 1. Study workflow reporting the sequential steps of the novel methodology used for the morphological characterisation of the GRF.

View, CA, USA) in order to characterise the GRF orientation with respect to the tibial plateau. The reconstructed model of the native knee before HTO was also used to fully plan the surgery and generate the surgical guide and fixation plate geometry for 3D printing.

2.4. HTO-TOKA® surgical technique

3D Metal Printing LTD (Bath, UK) developed a technology (TOKA® - Tailored Osteotomy Knee Alignment) to overcome the limits of the existing HTO treatment, which include the relatively small number of standard sizes of the fixation plate and the difficulty in achieving the desired correction. The TOKA® system comprises custom-made 3D printed surgical guide and fixation plate made in medical-grade titanium alloy (Ti-6Al-4 V). Both the anatomical fixation plate and the surgical guide are 3D-printed based on the subject's CT scans. This allows an improvement in the surgery accuracy along with a reduction of the surgical time [17]. Moreover, since the procedure is planned in advance based on the patient's morphology, it is less invasive with fewer intraoperative measurements and reduced need for multiple intra-operative radiological acquisitions.

2.5. Data processing

Relevant DICOM files were segmented using *Mimics* (Materialise NV, Leuven, Belgium) to reconstruct the morphological models of the proximal tibia and the additional markers. Then, the 3D bone model of the proximal tibia in STL format was imported in *Geomagic* (3D Systems, Rock Hill, SC-USA) to identify a number of landmarks through virtual palpation, necessary to define a tibial anatomical reference frame. The trajectories of the tibial markers acquired during GA were registered on

the corresponding coordinates from CT-based bone reconstruction. The registration matrices were estimated by implementing a Singular Value Decomposition algorithm [18]. As an intermediate step, the resulting matrices were used to report GRF data and the trajectory coordinates of the GA additional markers in the preliminary tibial reference frame. Then, the root mean square error (RMSE) was calculated to assess the marker cluster deformation and quantify the skin motion artefact. Finally, both the 3D model of the proximal tibia and the GRF and COP data were reported in the anatomical reference frame of the tibia, centred on the spine and defined according to [19]. A plane rigid with the tibial plateau was defined, based on three virtually palpated anatomical landmarks, i.e. the most lateral, medial and anterior points of the tibial plateau. The intersection point of each GRF vector throughout the stance phase was calculated for the examined limb, and produced intersection patterns at each repetition.

Within each pattern, those intersections associated to a number of relevant gait events were identified and highlighted, according to Benedetti et al. [20]: the two peaks of the vertical component of GRF, in the first and second half of the stance phase; the two peaks of the knee flex/ext moment and of the ab/adduction; and the single peak of the int/ext moment. As for the other motor tasks, the single moment peaks on the three anatomical planes were identified. All moments were normalised to percent patient's body weight times height. Joint rotations were calculated using internationally established recommendations [21].

Finally, to provide some preliminary quantitative evaluations about the outcomes of the surgery, the lateralisation of the GRF was calculated as the distance in mm between the pre- and post-operative patterns. All calculations were made in *Matlab* software package (version 2020b; The MathWorks, Inc., Natick, MA-USA).

3. Results

Pre-operative clinical and radiological scoring confirmed the diagnosis, i.e. medial knee osteoarthritis, with a maximum varus deformity of 13° over the patients.

To quantitatively characterise the GRF with respect to the proximal surface of the patient-specific tibial plateau, the GRF vectors were reported in the tibial anatomical reference frame, and the intersection points between these vectors and the plane defined by the three virtually palpated landmarks were calculated and depicted upon the tibial plateau morphology. As an example, the 3D model of the tibia depicted along with a GRF vector, selected among those collected during walking, is shown in Fig. 2 using data from a well representative patient.

Overall, this original procedure was successfully achieved both in pre-op and post-operative assessments with an acceptable level of error. As for this, cluster deformation was calculated to validate the procedure and quantify the skin motion artefact. In terms of RMSE, it resulted in approximately 2 mm error during walking and 3 mm for the other motor tasks.

Repeatable patterns of intersections between the GRF vectors and the proximal tibial plane (Fig. 3) were observed in the four analysed patients, although different before and after HTO and depending on the motor tasks. On average, corresponding standard deviations calculated over repetitions ranged from 8.8 mm to 15.2 mm before HTO; these values became 4.9 mm and 6.4 mm after HTO, indicating an increased data reproducibility after surgery.

During walking, before the surgery, the excessive varus resulted in medially located intersection patterns with respect to the tibial spine,

including those associated with the moments' peaks (Fig. 3). After HTO, these patterns were lateralised and much closer to the knee centre, as expected (Fig. 3). Furthermore, in order to assess the knee status during more demanding activities, one representative repetition before and one after HTO for the other motor tasks is reported in Fig. 4. Although the intersection patterns are different between the motor tasks, it was always confirmed the relevant lateralisation after HTO. To provide a quantitative evaluation of this modification, the medio-lateral position of the intersections associated with each significant moment's peak and to the pattern's centroid were calculated pre-op and post-HTO (Table 1). Relevant results, expressed both in mm and in percentage of the tibial plateau's width, show a general lateralisation, much marked in patient #2, i.e. that with the largest original deformity, equal to 13° varus, and thus subjected to the largest surgical correction via HTO.

Finally, the joint moments in the three planes were reported for walking both before and after HTO (Fig. 5) along with the corresponding control data [15]. After HTO, an overall restoration of the physiological knee moment patterns, especially the frontal one, was observed. Also in this case, this is much marked in patient #2.

4. Discussion and conclusion

The reported novel approach allows a linkage between kinetics data, including GRF, and the reconstructed 3D model of the tibial plateau. The procedure was successfully applied both before and after HTO, barring an acceptable level of error. The characterisation of the GRF on the tibial-plateau morphology was achieved pre- and post-operatively for the standard level walking and other more demanding motor tasks
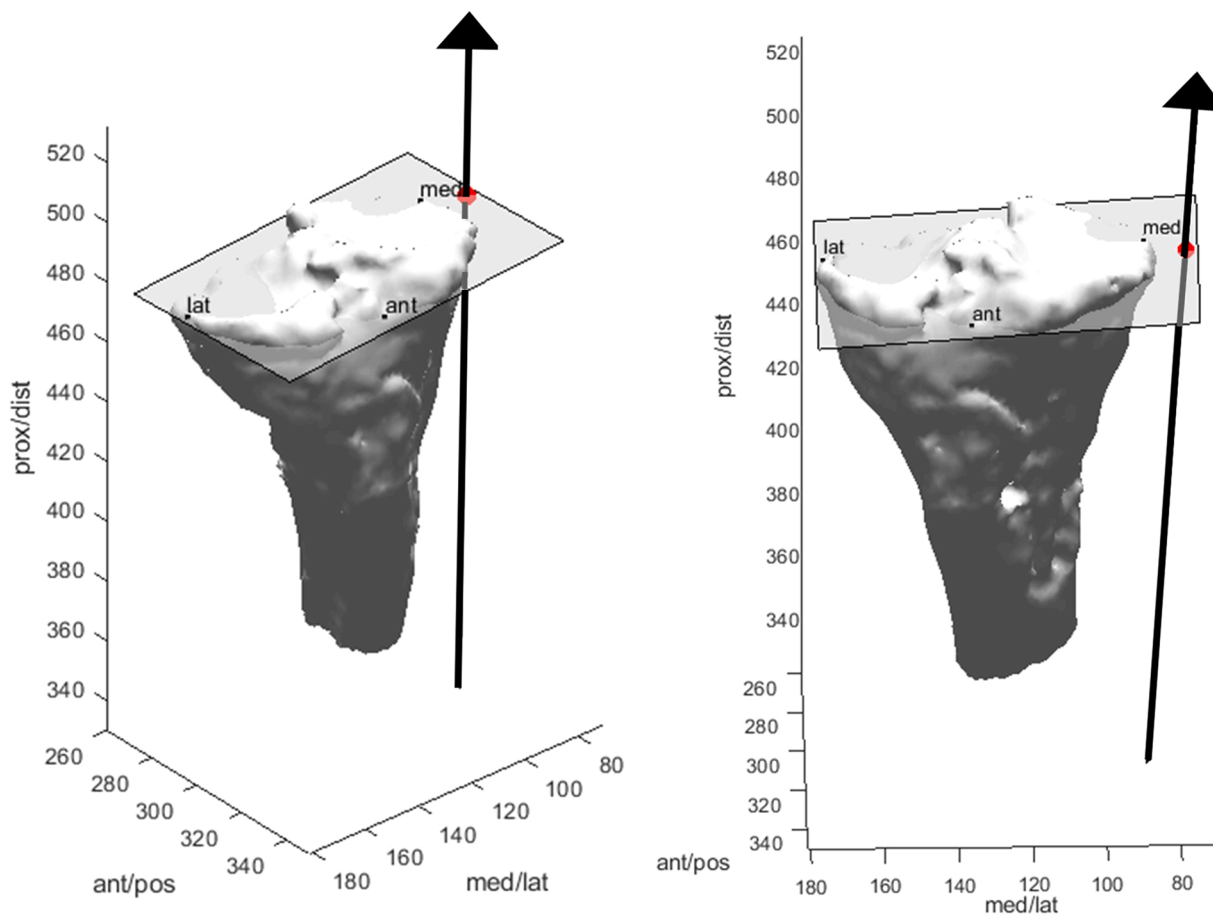

Fig. 2. 3D reconstructed model of the tibia reported in the GA laboratory reference frame along with the GRF vector (two arbitrary points of view of the same tibia and vector). The red dot represents the intersection point between the GRF vector and the plane passing through the proximal tibia. Data from a well representative patient.
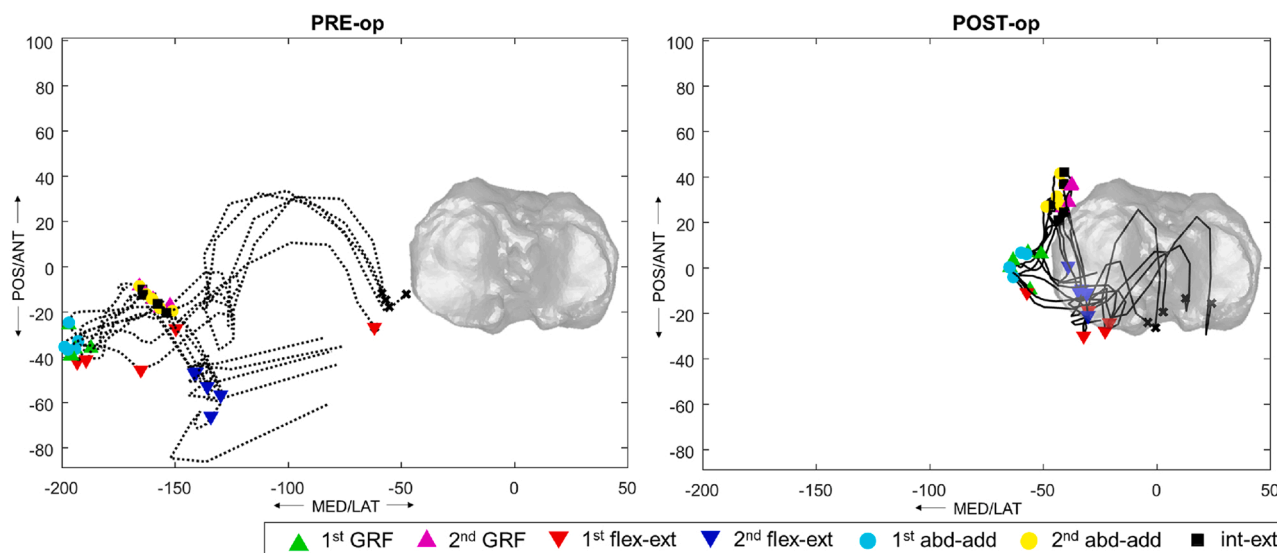
Fig. 3. Intersections patterns between the GRF vectors and the proximal tibial plane, during the stance phase of gait. Five repetitions during walking from the representative patient as in Fig. 2, before (left) and after (right) HTO. The intersection positions associated to the first and the second GRF peak in the stance phase (1st and 2nd GRF), to the first and the second sagittal (1st and 2nd flex-ext) and frontal (1st and 2nd abd-add) knee moment peaks, and to the transverse knee moment peak (int-ext) are pointed out.

requested in this study. Merging functional data from GA and the patient-specific 3D model of the tibial plateau permitted to characterise the position of the GRF at the knee level during motion.

The outcomes of the applied methodology confirmed the hypothesis: before HTO, the GRF was medially oriented with respect to the knee joint centre, as expected for a varus knee. This causes overloading and cartilage wear at the medial tibio-femoral compartment. Realigning the tibia, HTO resulted in the GRF moving laterally and closer to the tibial spine, thus restoring a more physiological loads distribution over the tibial plateau. The results were as expected but this study provides a direct proof in the achieved change in GRF orientation relative to the knee joint. The surgery improved the overall subjects' locomotion, which became more stable over time as demonstrated by higher repeatability in the intersection patterns after HTO. Also, relevant intersection points associated with force and moments peaks of the different repetitions within a single motor task formed a cluster, being located close to each other. This appeared much marked in the patient with the largest original deformity and, thus, subjected to the largest surgical correction via HTO.

The presented results were obtained using state-of-the-art GA techniques, along with reference frames, following ISB recommendations [21,22]. Also, a novel weight-bearing CT device was used to reconstruct the articular morphology. It allows a more realistic determination of the alignment of the articulation surfaces thus supporting the surgeon to produce a more reliable surgery planning. Compared to a traditional CT, it scans a bigger volume with a single rotation thus significantly reducing the acquisition time and the risk of image distortion caused by the patient movement. This results in more accurate and high resolution images with a lower radiation dose (~5–10 mGy) compared to standard CT systems (~20–50 mGy).

In the literature, several studies reported the correlation between a greater external KAM and increased loads on the medial compartment, often associated with the development of osteoarthritis. Therefore, the KAM has also been correlated with the bone distribution between the medial and lateral compartment of the tibial plateau that is, patients with narrow medial joint space have a greater peak of KAM [23]. Also, it is considered a surrogate measure of the medial tibiofemoral contact force. When the force vector passes medially to the tibial spine, it creates an adduction moment that is thought to increase load in the medial compartment [24,25]. Despite that, it is not reported how KAM affects

the morphology of interest in the case of lower limbs with varus deformity.

In their work [13], Whatling et al. reported the COP location measured relative to the foot and the knee. HTO moved the COP laterally compared to the pre-operative location, as expected. Nevertheless, they only reported the COP location at the timing of the first and second peak of the KAM, not the entire pattern, and the foot and tibial plateau illustration were not subject-specific. Also, no information about the location of the GRF relative to the knee was reported.

In this work, a patient-specific characterisation of the GRF on the tibial plateau was achieved and data were reported from the foot strike instance to the foot off.

This study suffers from some limitations. First, the reported cases are limited; this is because the multi-instrumental workflow makes the data extrapolation a demanding procedure and the data processing requires a considerable time, too. In the future, the present methodology will be applied to analyse a larger population of subjects. Therefore, a significant statistical analysis might be carried out to assess the outcomes of the surgery, to understand whether there are relevant differences between motor tasks and to find an index or a threshold to summarise the outcomes. Also, some sources of error could be the skin motion artefact and the patient movement during the CT acquisition, although they have not been observed.

In conclusion, in this work a novel procedure allowing a combination of motion data and patient-specific morphology was reported. It was proven that the articular realignment achieved with HTO is responsible for the transfer of loads closer to the knee centre. This is strictly related to medial compartment decompression, resulting in more physiological load distribution over the tibial plateau and, ideally, a slowdown of the progression of osteoarthritis.

Funding

Ethical Approval

This study was approved by the Ethics Committee (Prot. Gen. 0013355 on 30/10/2019) of the IRCCS Istituto Ortopedico, Bologna -
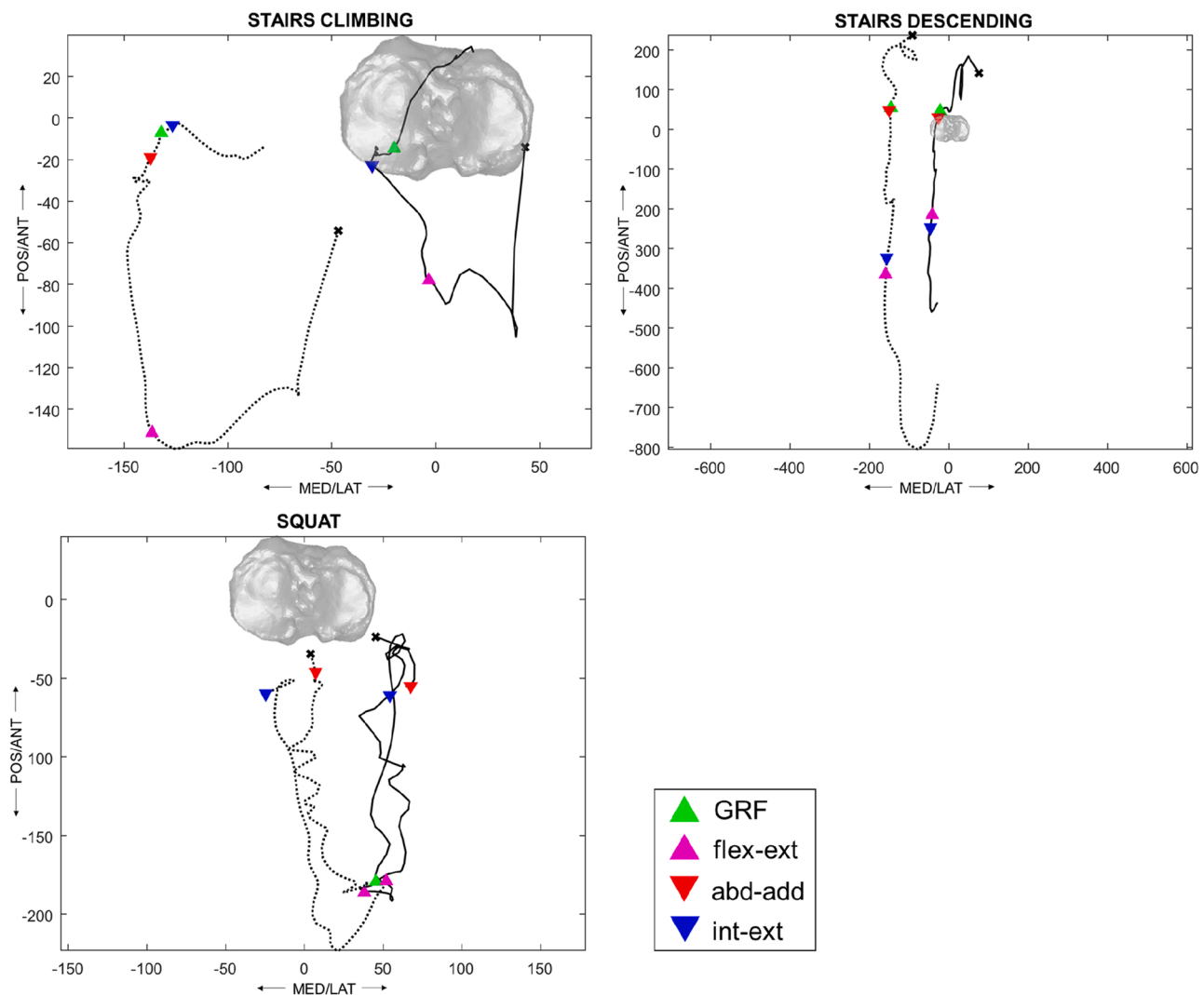
Fig. 4. Intersections patterns between the GRF vectors and the proximal tibial plane. One repetitions during demanding activities from the representative patient as in Fig. 2, before (dashed line) and after (solid line) HTO. The intersection positions associated to the GRF peak, and to the sagittal (flex-ext), frontal (abd-add) and transverse (int-ext) knee moment peaks are pointed out.

Italy (Cod. CE AVEC: 623/2019/Disp/IOR) and the clinical trial was registered at *ClinicalTrials.gov* (Cod.: NCT04574570). The authors certify that the institution approved the investigation protocol, that all investigations were conducted in conformity with ethical standard of research and in accordance with the relevant guidelines and regulations.

Consent

Signed Informed consent for participation in this study and to publish related anonymized information/images was obtained by all patients. All patients were above the age of 18 years.

CRediT authorship contribution statement

Miriana Ruggeri: Data curation, Formal analysis, Investigation, Methodology, Software, Validation, Visualization, Writing – original draft, Writing – review & editing. **Harinderjit Singh Gill**: Conceptualization, Formal analysis, Methodology, Validation, Writing – review & editing. **Alberto Leardini**: Conceptualization, Formal analysis, Funding acquisition, Project administration, Resources, Supervision, Validation, Writing – original draft, Writing – review & editing. **Stefano Zaffagnini**: Funding acquisition, Resources, Writing – review & editing. **Alisdair MacLeod**: Software, Visualization, Writing – review & editing.

Maurizio Ortolani: Data curation, Investigation, Software, Visualization, Writing – review & editing. **Federica Faccia**: Data curation, Investigation, Software, Visualization, Writing – review & editing. **Alberto Grassi**: Investigation, Writing – review & editing. **Giacomo Dal Fabbro**: Data curation, Investigation, Writing – review & editing. **Stefano Durante**: Data curation, Investigation, Project administration, Software, Visualization, Writing – review & editing. **Claudio Belvedere**: Conceptualization, Formal analysis, Investigation, Methodology, Project administration, Supervision, Validation, Writing – original draft, Writing – review & editing.

Authorship

All authors have made substantial contributions to the conception and design of the study, or acquisition of data, or analysis and interpretation of data. They also have made substantial contributions to drafting the article or revising it critically for important intellectual content, as well as to the final approval of the submitted version. Due to the very interdisciplinary nature of the present work, which involved biomedical and mechanical engineers, orthopaedic surgeons, radiographers, IT laboratory specialists, the author list has been extended to more than eight authors in order to include all those whose experties were necessary for the study and who provided also substantial

Table 1

Medio-lateral position (in mm) of the intersections points between the GRF vectors and the proximal tibial plane associated to the knee moment peaks and pattern centroids before (PRE) and after (POST) HTO. The difference between these two conditions is reported both in mm and in percentage (%) of the tibial plateau's width. Abbreviations as in Fig. 3 for the walking task and as in Fig. 4 for the demanding motor tasks.

|		# 1				# 2				# 3				# 4			
		Position (mm)		Difference		Position (mm)		Difference		Position (mm)		Difference		Position (mm)		Difference	
		PRE	POST	mm	%	PRE	POST	mm	%	PRE	POST	mm	%	PRE	POST	mm	%
Walking	1st GRF	-86.8	-55.5	31.4	40.2	-169.0	-53.0	115.9	126.4	-99.1	-43.4	55.7	77.5	-166.8	-46.2	120.5	144.5
	2nd GRF	-106.3	-60.7	45.6	58.4	-179.5	-47.1	132.4	144.4	-105.3	-37.8	67.5	93.8	-149.1	-43.8	105.3	126.3
	1st flex/ext	-72.6	-14.6	58.1	74.3	-126.4	-0.5	125.9	137.3	-99.1	-43.4	55.7	77.5	-163.9	-60.5	103.3	123.9
	2nd flex/ext	-97.8	-58.5	39.3	50.3	-171.5	-45.7	125.8	137.2	-98.8	-30.7	68.1	94.8	-133.5	-42.5	91.0	109.1
	1st abd/add	-81.3	-57.4	23.9	30.6	-169.0	-49.6	119.4	130.2	-93.2	-38.5	54.8	76.2	-148.1	-44.2	103.9	124.6
	2nd abd/add	-105.6	-60.7	44.9	57.5	-180.5	-46.3	134.2	146.4	-104.9	-37.8	67.1	93.3	-159.1	-43.5	115.6	138.6
	int/ext rot	-101.3	-60.0	41.3	52.9	-177.9	-46.3	131.6	143.5	-104.1	-35.9	68.1	94.8	-151.5	-43.6	108.0	129.5
	centroid	-88.5	-54.5	34.0	43.6	-160.5	-39.6	120.9	131.9	-90.4	-25.4	65.0	90.4	-136.4	-38.3	98.1	117.6
Stairs descending	GRF	-117.0	-43.8	73.3	93.8	-145.4	-21.3	124.1	135.3	-32.5	-13.8	18.7	26.0	-117.4	43.0	160.4	192.3
	flex/ext	-135.9	-52.2	83.8	107.3	-158.8	-41.8	117.0	127.6	-122.6	0.7	123.3	171.5	-19.0	43.0	61.9	74.2
	abd/add	-100.0	-29.6	70.4	90.1	-150.7	-27.2	123.5	134.6	-37.5	-14.4	23.1	32.1	-104.5	16.7	121.2	145.4
	int/ext rot	-131.5	-50.3	81.1	103.9	-157.1	-46.4	110.6	120.6	-104.7	-12.1	92.6	128.7	-101.8	16.1	117.8	141.3
	centroid	-114.0	-27.8	86.2	110.4	-142.3	-26.0	116.3	126.8	-82.0	-3.7	78.4	109.0	-85.8	41.0	126.8	152.1
Stairs climbing	GRF	-110.7	-34.5	76.3	97.6	-132.2	-19.9	112.3	122.5	-47.2	14.5	61.7	85.8	-75.0	-14.6	60.4	72.4
	flex/ext	-111.9	-33.9	77.9	99.8	-136.5	-4.1	132.5	144.4	-88.7	-1.3	87.4	121.6	-144.8	6.9	151.7	181.8
	abd/add	-96.3	-46.9	49.4	63.2	-137.5	-31.0	106.5	116.1	-92.1	-0.8	91.4	127.1	-150.9	-26.2	124.6	149.4
	int/ext rot	-91.5	-40.8	50.7	64.9	-126.7	-31.0	95.7	104.3	-92.1	-2.0	90.2	125.4	-150.9	-26.2	124.6	149.4
	centroid	-88.6	-28.2	60.4	77.3	-127.0	-10.6	116.3	126.9	-66.2	8.5	74.7	103.9	-111.8	-4.0	107.8	129.3
Squat	GRF	-31.2	-28.5	2.8	3.5	44.9	37.7	-7.2	-7.8	48.7	45.0	-3.8	-5.3	-25.0	40.6	65.6	78.7
	flex/ext	-31.6	-29.5	2.1	2.7	52.1	37.7	-14.4	-15.7	60.9	37.6	-23.3	-32.4	-49.9	29.3	79.2	95.0
	abd/add	-21.3	20.4	41.7	53.4	6.2	70.2	64.0	69.8	46.6	56.6	10.0	13.8	-41.6	20.9	62.5	74.9
	int/ext rot	10.6	19.1	8.4	10.8	-24.7	56.0	80.7	88.0	64.7	21.7	-42.9	-59.7	-28.9	45.1	74.1	88.8
	centroid	-32.4	2.3	34.7	44.5	12.6	54.4	41.7	45.5	56.6	50.6	-6.0	-8.3	-19.2	39.2	58.4	70.0
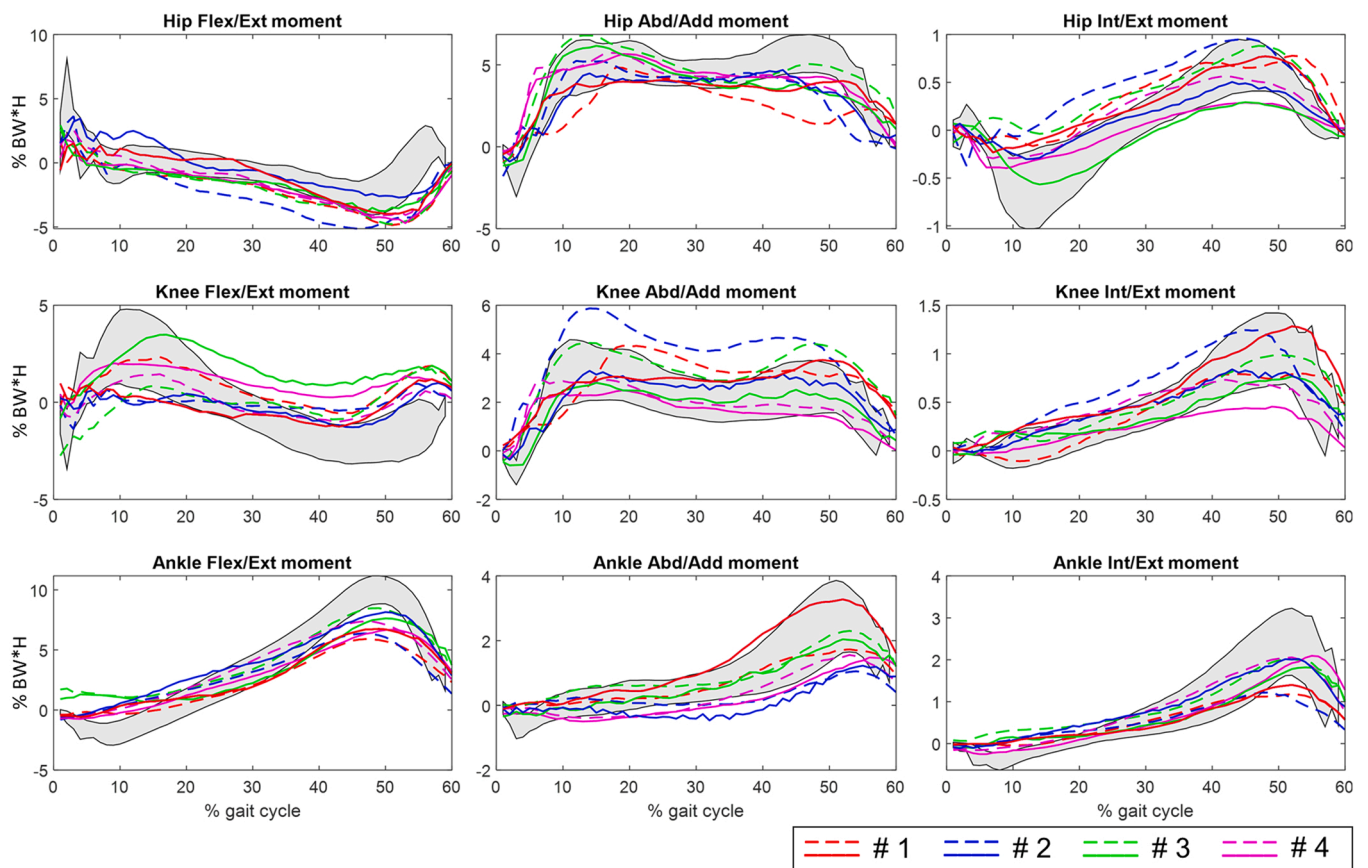
Fig. 5. Joint moments during walking before (dashed line) and after (solid line) HTO. Data were normalised to percent patient's body weight (BW) times height (H).

contributions to the present manuscript.

Declarations of interest

None.

Data availability

The datasets used and/or analysed during the current study are available from the corresponding author on reasonable request.

References

[1] L. Sharma, J. Song, D. Dunlop, D. Felson, C.E. Lewis, N. Segal, et al., Varus and valgus alignment and incident and progressive knee osteoarthritis, Ann. Rheum. Dis. 69 (11) (2010) 1940–1945.

[2] A.J. Baliunas, D.E. Hurwitz, A.B. Ryals, A. Karrar, J.P. Case, J.A. Block, et al., Increased knee joint loads during walking are present in subjects with knee osteoarthritis, Osteoarthr. Cartil. 10 (7) (2002) 573–579.

[3] D. Moschella, A. Blasi, A. Leardini, A. Ensini, F. Catani, Wear patterns on tibial plateau from varus osteoarthritic knees, Clin. Biomech. 21 (2) (2006) 152–158.

[4] L. Sharma, The role of varus and valgus alignment in knee osteoarthritis, Arthritis Rheum. 56 (4) (2007) 1044–1047. ⟨https://www.ncbi.nlm.nih.gov/pubmed/173 93411⟩.

[5] D.C. Lee, S.J. Byun, High tibial osteotomy, Knee Surg. Relat. Res. 24 (2) (2012) 61–69.

[6] R. Rossi, D.E. Bonasia, A. Amendola, The role of high tibial osteotomy in the Varus Knee, JAAOS J. Am. Acad. Orthop. Surg. 19 (10) (2011) 590–599. ⟨https://journa ls.lww.com/jaaos/Fulltext/2011/10000/The_Role_of_High_Tibial_Osteotomy_in _the_Varus.3.aspx⟩.

[7] J.P. Jackson, W. Waugh, Tibial osteotomy for osteoarthritis of the knee, J. Bone Jt. Surg. Br. 43-b (1961) 746–751.

[8] Y. Fujisawa, K. Masuhara, S. Shiomi, The effect of high tibial osteotomy on osteoarthritis of the knee. An arthroscopic study of 54 knee joints, Orthop. Clin. N. Am. 10 (3) (1979) 585–608.

[9] T. Nagura, Y. Niki, K. Harato, Y. Kuroyanagi, Y. Kiriyama, T. Mochizuki, et al., Increased medially oriented ground reaction force during gait in patients with varus knee osteoarthritis can be treat target to reduce medial compartment loads,

[10] Osteoarthr. Cartil. 22 (2014) S122–S123, https://doi.org/10.1016/j. joca.2014.02.223.

[10] K.L. Bennell, K.A. Bowles, Y. Wang, F. Cicuttini, M. Davies-Tuck, R.S. Hinman, Higher dynamic medial knee load predicts greater cartilage loss over 12 months in medial knee osteoarthritis, Ann. Rheum. Dis. 70 (10) (2011) 1770–1774.

[11] A. Navacchia, P.J. Rullkoetter, P. Schütz, R.B. List, C.K. Fitzpatrick, K.B. Shelburne, Subject-specific modeling of muscle force and knee contact in total knee arthroplasty, J. Orthop. Res. 34 (9) (2016) 1576–1587. ⟨https://onlinelibrary. wiley.com/doi/abs/10.1002/jor.23171⟩.

[12] I. Loi, D. Stanev, K. Moustakas, Total knee replacement: subject-specific modeling, finite element analysis, and evaluation of dynamic activities, Front. Bioeng. Biotechnol. 9 (2021). ⟨https://www.frontiersin.org/article/10.3389/fbioe.2021. 648356⟩.

[13] G.M. Whatling, P.R. Biggs, D.W. Elson, A. Metcalfe, C. Wilson, C. Holt, High tibial osteotomy results in improved frontal plane knee moments, gait patterns and patient-reported outcomes, Knee Surg. Sports Traumatol. Arthrosc. 28 (9) (2020) 2872–2882. ⟨https://www.ncbi.nlm.nih.gov/pubmed/31384981⟩.

[14] Y. Dai, J.E. Bischoff, Comprehensive assessment of tibial plateau morphology in total knee arthroplasty: influence of shape and size on anthropometric variability, J. Orthop. Res. 31 (10) (2013) 1643–1652. ⟨https://onlinelibrary.wiley.com/doi/ abs/10.1002/jor.22410⟩.

[15] A. Leardini, Z. Sawacha, G. Paolini, S. Ingrosso, R. Nativo, M.G. Benedetti, A new anatomically based protocol for gait analysis in children, Gait Posture 26 (4) (2007) 560–571. ⟨https://www.ncbi.nlm.nih.gov/pubmed/17291764⟩.

[16] A. Leardini, F. Biagi, C. Belvedere, M.G. Benedetti, Quantitative comparison of current models for trunk motion in human movement analysis, Clin. Biomech. 24 (7) (2009) 542–550. ⟨https://www.ncbi.nlm.nih.gov/pubmed/19482392⟩.

[17] A. MacLeod, C. Belvedere, G. Dal Fabbro, A. Grassi, G. Nervuti, A. Leardini, et al., First clinical experience of a personalised 3d-printed osteotomy system for knee arthritis treatment, British Orthopaedic Research Society Annual Meeting, Conference Proceedings of BORS, Online, 2021.

[18] I. Söderkvist, P.A. Wedin, Determining the movements of the skeleton using well-configured markers, J. Biomech. 26 (12) (1993) 1473–1477.

[19] E.S. Grood, W.J. Suntay, A joint coordinate system for the clinical description of three-dimensional motions: application to the knee, J. Biomech. Eng. 105 (2) (1983) 136–144. ⟨https://www.ncbi.nlm.nih.gov/pubmed/6865355⟩.

[20] M.G. Benedetti, F. Catani, A. Leardini, E. Pignotti, S. Giannini, Data management in gait analysis for clinical applications, Clin. Biomech. 13 (3) (1998) 204–215.

[21] G. Wu, S. Siegler, P. Allard, C. Kirtley, A. Leardini, D. Rosenbaum, et al., ISB recommendation on definitions of joint coordinate system of various joints for the

reporting of human joint motion–part I: ankle, hip, and spine. International Society of Biomechanics, J. Biomech. 35 (4) (2002) 543–548.

[22] G. Wu, P.R. Cavanagh, ISB recommendations for standardization in the reporting of kinematic data, J. Biomech. 28 (10) (1995) 1257–1261.

[23] D.E. Hurwitz, A.B. Ryals, J.P. Case, J.A. Block, T.P. Andriacchi, The knee adduction moment during gait in subjects with knee osteoarthritis is more closely correlated with static alignment than radiographic disease severity, toe out angle and pain, J. Orthop. Res. 20 (1) (2002) 101–107.

[24] I. Kutzner, A. Trepczynski, M.O. Heller, G. Bergmann, Knee adduction moment and medial contact force – facts about their correlation during gait, PLoS One 8 (12) (2013), e81036, https://doi.org/10.1371/journal.pone.0081036.

[25] O.D. Schipplein, T.P. Andriacchi, Interaction between active and passive knee stabilizers during level walking, J. Orthop. Res. 9 (1) (1991) 113–119.